Available online at www.sciencedirect.com

SCIENCE DIRECT

Developmental Biology 294 (2006) 24–38

DEVELOPMENTAL BIOLOGY

www.elsevier.com/locate/ydbio

NAADP and $InsP_3$ play distinct roles at fertilization in starfish oocytes

Francesco Moccia [a,*], Gilda A. Nusco [a], Dmitry Lim [a,1], Keiichiro Kyozuka [b], Luigia Santella [a]

[a] *Laboratory of Cell Signaling, Stazione Zoologica "Anton Dohrn", Villa Comunale, 80121 Naples, Italy*
[b] *Asamushi Marine Biological Station, Aomori 039-3501, Japan*

Received for publication 16 September 2005; revised 6 February 2006; accepted 14 February 2006
Available online 20 March 2006

Abstract

NAADP participates in the response of starfish oocytes to sperm by triggering the fertilization potential (FP) through the activation of a Ca^{2+} current which depolarizes the membrane to the threshold of activation of the voltage-gated Ca^{2+} channels. The aim of this study was to investigate whether this Ca^{2+} influx is linked to the onset of the concomitant $InsP_3$-mediated Ca^{2+} wave by simultaneously employing Ca^{2+} imaging and single-electrode intracellular recording techniques. In control oocytes, the sperm-induced membrane depolarization always preceded by a few seconds the onset of the Ca^{2+} wave. Strikingly, the self-desensitization of NAADP receptors either abolished the Ca^{2+} response or resulted in abnormal oocyte activation, i.e., the membrane depolarization followed the Ca^{2+} wave and the oocyte was polyspermic. The inhibition of $InsP_3$ signaling only impaired the propagation of the Ca^{2+} wave and shortened the FP. The duration of FP was also reduced in low-Na^+ sea water. Finally, uncaged $InsP_3$ produced a Ca^{2+} increase, which depolarized the membrane upon the activation of a Ca^{2+}-sensitive cation current. These results support the hypothesis that Ca^{2+} entry during the NAADP-triggered FP is required for the onset of the Ca^{2+} wave at fertilization. The $InsP_3$-mediated Ca^{2+} wave, in turn, may interact with the NAADP-evoked depolarization by activating a Ca^{2+}-dependent Na^+ entry.

Keywords: NAADP; $InsP_3$; Ca^{2+} wave; Fertilization; Oocytes; Sperm; Starfish

Introduction

The sperm signals the resumption of the cell cycle and the start of the embryonic development in inseminated oocytes by stimulating a massive increase in intracellular Ca^{2+}. A proper Ca^{2+} signal results in the temporally-regulated activation of the Ca^{2+}-sensitive effectors of the differentiation program that eventually leads to the genesis of a new organism (Santella et al., 2004). The Ca^{2+} increase at fertilization may occur as a single Ca^{2+} transient or repetitive Ca^{2+} oscillations (Stricker, 1999) and is accompanied by a positive shift in the membrane potential (V_m), the so-called fertilization potential (FP). The FP consists of a sperm-induced initial depolarization that may be amplified by an action potential (AP) driven by voltage-gated Ca^{2+} channels, which results in a transient ring of brightness beneath the membrane (cortical flash) and protects the eggs from polyspermy during the first minutes after insemination (fast block) (Gould and Stephano, 2003; Santella et al., 2004). When the membrane repolarizes, a slower mechanical block to polyspermy is established by the Ca^{2+}-dependent exocytosis of cortical granules, which permits a normal embryonic development (Gould and Stephano, 2003).

The Ca^{2+} signal at fertilization in deuterostomes mainly relies on the inositol 1,4,5-trisphosphate ($InsP_3$)-sensitive domain of the endoplasmic reticulum (ER) (Runft et al., 2002). The contribution of ryanodine receptors (RyRs) has been shown only in sea urchin eggs, where they are activated by cyclic ADP-ribose (cADPr) (Lee et al., 1993; Stricker, 1999). The role of Ca^{2+} entry in sustaining the Ca^{2+} discharge is still a matter of debate in echinoderms (Runft et al., 2002). Crèton and Jaffe (1995) have demonstrated that Ca^{2+} influx during the latent period between the Ca^{2+}-AP and the Ca^{2+} wave is required for egg activation in sea urchin. However, this evidence has been underestimated by several authors (Runft et al., 2002), as these eggs can be activated by reacted sperm in a low-Ca^{2+} medium (McDougall et al., 1993). Nevertheless, in prophase I-arrested oocytes, the FP-dependent Ca^{2+} influx may

* Corresponding author. Fax: +39 81 7641355.
E-mail address: moccia@szn.it (F. Moccia).
[1] Current address: Department of Biochemistry, University of Padova, Viale G. Colombo 3, 35121 Padova, Italy.

0012-1606/$ - see front matter © 2006 Elsevier Inc. All rights reserved.
doi:10.1016/j.ydbio.2006.02.011

participate in oocyte activation (Santella et al., 2004). Consistently, in molluscs and echiurans, the cortical flash spreads centripetally without recruiting either $InsP_3$ receptors ($InsP_3Rs$) or RyRs (Deguchi and Morisawa, 2003; Stephano and Gould, 1997). Moreover, in annelids, the sperm-promoted membrane depolarization initiates the Ca^{2+} spiking that activates the eggs (Eckberg and Miller, 1995).

Scarce information is available on the trigger of the sperm-evoked initial depolarization, which has been unravelled only in a few species. Recent studies indicate that nicotinic acid adenine dinucleotide phosphate (NAADP) may gate the fertilization channel in starfish oocytes (Moccia et al., 2004). The NAADP-sensitive current is mainly carried by Ca^{2+}, but not by Na^+, displays an inwardly-rectifiying I–V relationship, and is insensitive to the inhibition of either $InsP_3Rs$ or RyRs (Moccia et al., 2003a). Moreover, unlike the NAADP receptor described in sea urchin (Churchill et al., 2002a), the response to NAADP in starfish oocytes is unaffected by the impairment of lysosomal function with either bafilomycin A1 or glycyl-L-phenylalanine-β-naphrylamide (GPN; unpublished observations from our lab). In agreement with the role of NAADP in triggering the FP in starfish, the injection of NAADP elicits a cortical Ca^{2+} flash which is not affected by the down-regulation of $InsP_3Rs$ (Santella et al., 2000; Lim et al., 2001).

Due to their large size, transparency and easy handling, starfish oocytes provide a suitable model to investigate the interaction between the external Ca^{2+}-dependent cortical flash and the intracellular Ca^{2+} wave at fertilization (Lim et al., 2001; Santella et al., 2002). In addition to the NAADP-dependent Ca^{2+} channels on the plasma membrane (Moccia et al., 2003a), starfish oocytes possess functional $InsP_3Rs$ and RyRs (Lim et al., 2001; Nusco et al., 2002), which mediate a massive Ca^{2+} release from the ER. Moreover, unlike sea urchin which undergoes post-meiotic fertilization, starfish displays a more typical developmental mode in which fertilization occurs before meiosis is completed. Indeed, immature oocytes arrested at the germinal vesicle (GV; nucleus) stage (prophase I) resume the cell cycle in vitro upon exposition to the maturation-inducing hormone, 1-methyladenine (1-MA) (Santella and Kyozuka, 1994; Santella et al., 2005). During maturation, oocytes undergo several biochemical, morphological and electrophysiological changes, including an increase in $InsP_3Rs$ sensitivity (Lim et al., 2003) and in input resistance (R_{input}) (Moccia et al., 2004). As a consequence of meiosis resumption, the oocytes may undergo monospermic fertilization, which normally occurs between metaphase I and the extrusion of the first polar body (Meijer and Guerrier, 1984). In response to the sperm, the oocyte manifests an $InsP_3$-dependent single-source Ca^{2+} wave, which may be either preceded or followed by the cortical flash (Moccia et al., 2003a; Nusco et al., 2002; Stricker, 1999). As mentioned above, NAADP triggers the FP through the activation of a Ca^{2+}-mediated inward current (Moccia et al., 2003a, 2004). The involvement of NAADP in the fertilization process of starfish and sea urchin eggs has been corroborated by the finding that: (1) sea urchin sperms produce NAADP (Billington et al., 2002) and (2) a bolus of NAADP delivered into sea urchin eggs may trigger the cortical flash (Churchill et al., 2003). Although the Ca^{2+} pulse from NAADP receptors is amplified by $InsP_3Rs$ during the response to physiological agonists in mammalian cells (Cancela, 2001; Yamasaki et al., 2005; Santella, 2005), it is still unknown whether NAADP-dependent Ca^{2+} influx plays a role in triggering the $InsP_3$-mediated Ca^{2+} wave at fertilization in echinoderms (Lim et al., 2001). Investigating whether NAADP-elicited Ca^{2+} entry and $InsP_3$-induced Ca^{2+} release are two mechanistically related events would help identify the initial signaling pathway that leads to oocytes activation (Runft et al., 2002).

In the present study, we have simultaneously measured the changes in both V_m and intracellular Ca^{2+} level during the fertilization of starfish oocytes. Our main goal was to assess the role of NAADP in the onset of the intracellular Ca^{2+} response upon sperm binding. We provide the evidence that desensitization of NAADP receptors either prevents Ca^{2+} release or impairs the pattern of oocyte activation. Thus, Ca^{2+} influx during the early phase of the NAADP-induced FP plays a role in the initiation of the Ca^{2+} wave at fertilization. $InsP_3$, in turn, may boost the initial NAADP-dependent depolarization and maintain the FP through the activation of Ca^{2+}-sensitive Na^+ influx. In contrast, the cADPr-dependent RyRs do not contribute to either the membrane depolarization or the Ca^{2+} increase.

Materials and methods

Preparation of oocytes

Starfish (*Astropecten auranciacus*) were collected during the breeding season in February-April in the Gulf of Naples and maintained in running natural sea water (16°C). Fully grown immature oocytes were harvested from the ovaries and washed in filtrated artificial sea water (ASW: 500 mM NaCl, 8 mM KCl, 10 mM $CaCl_2$, 12 mM $MgCl_2$, 2.5 mM $NaHCO_3$, pH 8.0 titrated with NaOH) 40–50 min before use. Maturation was promoted by adding 10 μM 1-MA (Sigma Chemicals Co., St. Louis, MO).

Microinjections and Ca^{2+} imaging

The calcium fluorescent dye Calcium Green-1 coupled to a 10-kDa dextran (CG, Molecular Probes, Eugene, Ore., USA) was injected into the cytoplasm of immature oocytes by pressure, using an Eppendorf Transjector 5246, at a concentration of 5 mg/ml in the injection buffer (450 mM potassium chloride, 10 mM HEPES, pH 7.4). NAADP, Heparin, 8-NH_2-cADPr, ryanodine and ruthenium red were injected into mature oocytes at the concentrations of 1 μM, 50 mg/ml, 400 μM, 2 mM and 100 μM in the injection buffer, respectively. As the volume of the injected substances corresponded to 1–2% of the oocyte volume, their final concentration inside the cells was estimated 50–100 times lower than in the micropipette. For the experiments with the caged compounds, the solutions in the pipette contained 10 μM $InsP_3$ or 100 μM NAADP.

Cytosolic Ca^{2+} changes were measured every 500 ms with a cooled CCD camera (Coolsnap HQ, Princeton Instruments, Inc., Trenton, NJ) mounted on a Zeiss Axiovert 100 microscope endowed with a Plan-Neofluar 20×/0.50 objective. The sampling rate was decreased to 1 image every 5 s after completion of the Ca^{2+} wave due to the storage limit of the personal computer. The caged compounds were photolysed by irradiating the oocytes with ultraviolet (UV) light (330 nm) emitted by a computer-controlled shutter (Lambda 10-2, Sutter Instruments, Co., Novato, CA). Fluorescence images were processed with a MetaMorph Imaging System software (Universal Imaging Corporation, West Chester, PA). In order to exclude background fluorescence, the fluorescence level detected after the onset of the response was normalized against baseline fluorescence and the images were displayed in terms of relative fluorescence $F_{rel} = [(f_t - f_0)/f_0]$, where f_t is the recorded fluorescence and f_0 is the resting

fluorescence before the onset of the response. The changes in fluorescence level were measured by using the oocyte pixels within a region of interest (ROI) drawn around the cell whose fluorescent intensity rose above a threshold value set at f_0 (Moccia et al., 2003b).

Electrophysiology

Intracellular recordings were performed by impaling mature oocytes with sharp glass electrodes (filament type, 1.5 mm o.d.; Harvard Apparatus, U.K.), which were filled with 450 mM KCl and had a resistance of 40–50 MΩ. The microelectrodes were pulled by using a Sutter Instrument P-87 pipette puller. The impalement was obtained by applying short current pulses through the electrode until V_m became steady around a negative value. Only oocytes whose resting V_m remained stable within ±3 mV at least 10 min after the impalement were inseminated. The V_m was recorded through a headstage connected to an Axoclamp-2B amplifier (Axon Instruments Inc., Union City, CA) in bridge mode (Moccia et al., 2004). The changes in V_m induced by either the sperm or the caged compounds were sampled at 1 kHz and digitized with a Digidata 1200B data acquisition system. R_{input} was measured by injecting hyperpolarizing current pulses to induce steady state voltage response between 3 and 15 mV (Goudeau et al., 1992). The oocytes were always bathed in ASW. To investigate if the FP depends on extracellular Na^+, 495 mM NaCl was replaced by an equimolar amount of choline chloride (Na^+-FreeSW). Experiments were carried out at room temperature (20–23°C).

Statistics

Pooled data were given as means ± Standard Error (SE) and the significance of differences between the averages was evaluated by Student's *t* test for paired or unpaired observations. $P < 0.05$ was considered significant. The cells could be divided into two groups, depending on the value of R_{input} (see below). The measured parameters of the FP and the Ca^{2+} increase did not display significant difference among oocytes with low and high R_{input} and, therefore, were pooled together for the sake of clarity, unless it was stated otherwise.

Reagents

Caged $InsP_3$ and NAADP were purchased from Calbiochem (La Jolla, CA) and Molecular Probes, respectively. All the other chemicals were of analytical grade and obtained from Sigma Chemical Co.

Results

Electrical properties of unfertilized mature starfish oocytes

Before investigating the role of NAADP-induced Ca^{2+} entry in the onset of intracellular Ca^{2+} release at fertilization, we evaluated the membrane electrical properties of unfertilized oocytes, the background upon which the fertilization events are superimposed. It has been reported that resting V_m may dramatically vary from cell to cell when mature starfish oocytes are bathed in ASW and impaled with one microelectrode (Miyazaki et al., 1975; Miyazaki and Hirai, 1979). Accordingly, the values of resting V_m of unfertilized mature oocytes ranged between −100 mV and −1 mV (see Materials and methods) and could be fitted by a bimodal distribution peaking at −73.3 ± 1.8 mV ("high V_m") and −13.8 ± 3.5 mV ("low V_m"). These numbers are also within the same range as those reported in sea urchin (McCulloh et al., 1987). R_{input} of mature oocytes was measured after stabilization of the resting potential and ranged between 60 MΩ and 1530 MΩ, averaging 267.1 ± 250.8 MΩ ($n = 66$). The rationale behind the scattering in R_{input}, which was not correlated with that in the resting V_m ($r = 0.00845$), will be clarified below. The large variation in the resting potential likely results from a leakage current due to a damage caused by electrode penetration, which may produce an artifictual membrane potential drop in "low V_m" cells (Moccia et al., 2004). Furthermore, an increase in Na^+ permeability during maturation could induce a membrane depolarization in some cells (Miyazaki et al., 1975; Moccia et al., 2004). Although it has been reported that Ca^{2+} entry during the Ca^{2+}-AP upstroke results in the cortical flash observed in oocytes from several species (Santella et al., 2004; Stricker, 1999), this feature has never been directly assessed in starfish oocytes. Therefore, we first recorded the subcellular profile of the Ca^{2+} signal elicited by the regenerative process with a cooled CCD camera. In oocytes held at −71.2 ± 0.7 mV ($n = 18$) by applying a steady-state negative current to "low V_m" cells, short depolarizing current pulses induced a Ca^{2+}-AP, which triggered at −59.7 ± 1.5 mV ($n = 18$), overshot zero by +5.9 ± 3.5 mV ($n = 17$) and lasted 8.0 ± 1.9 s ($n = 16$) (blue trace in Fig. 1B). Notably, the peak of the regenerative response (blue arrow in Fig. 1B) caused a cortical Ca^{2+} flash (green arrows in Figs. 1A and B), which did not spread inwardly (see the second relative fluorescence image in Fig. 1A) and lasted 9.2 ± 1.8 s ($n = 10$) (green trace in Fig. 1B). Accordingly, both the AP and the cortical flash disappeared in Ca^{2+}-free seawater ($n = 4$, data not shown).

The onset of the membrane depolarization precedes the Ca^{2+} wave at fertilization

Since fertilization physiologically occurs at V_m near −70 mV in echinoderms (Miyazaki and Hirai, 1979), the

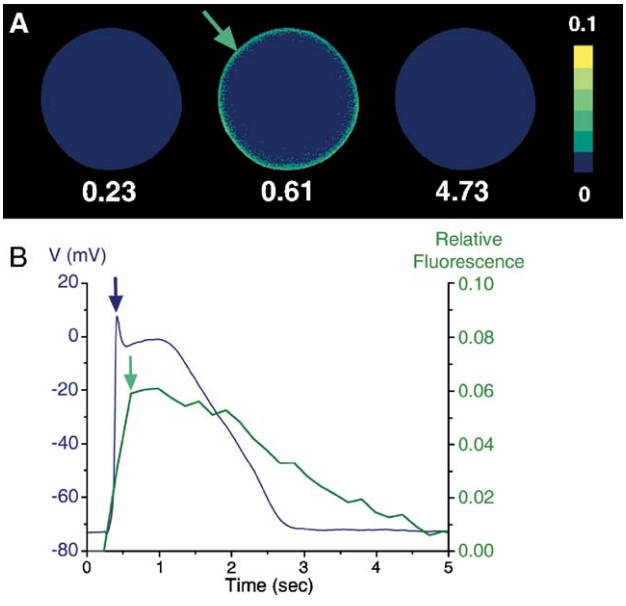

Fig. 1. The Ca^{2+}-AP produces a cortical flash in starfish oocytes. (A) Ca^{2+} inflow during the AP upstroke results in a cortical flash (green arrow) which does not centripetally spread in an unfertilized mature oocyte. (B) The blue trace depicts the time courses of the AP, while the green trace tracks the simultaneous cortical Ca^{2+} increase. In this and the following figures, the peak of the Ca^{2+}-AP and the cortical flash are indicated by a blue and a green arrow, respectively.

oocytes were inseminated at −73.0 ± 0.8 mV (n = 74). The first detectable response to the fertilizing sperm was a membrane depolarization, which marked the time of sperm–oocyte fusion (Miyazaki and Hirai, 1979). In 29 out of 74 oocytes, the shift in V_m arose abruptly, forming a step of 4.6 ± 0.6 mV (n = 26) above the baseline (sperm symbol in Fig. 2B). The voltage step was followed by a "pacemaker"-like depolarization, which reached the threshold of the regenerative process (−55.9 ± 2.3 mV, n = 26) after 6.5 ± 0.6 s (n = 26) (red circle in Fig. 2B). In the remaining 45 oocytes, the initial depolarization was higher (≈8–10 mV), faster (300–500 ms) and reached the threshold of the AP, which was set at a significantly higher potential (−65.6 ± 1.4 mV, n = 45; P = 0.00035), without forming a step (blue trace in Fig. 2F). Whatever the pattern of the initial depolarization is, the regenerative process overshot zero by +12.7 ± 1.7 mV (n = 70) (blue arrows in Figs. 2A and E), rapidly decayed to a "well" of −19.6 ± 2.1 mV (n = 74), and was followed by a slower voltage shift which attained a maximum level of +10.1 ± 1.3 mV (n = 70) after 76.7 ± 6.5 s

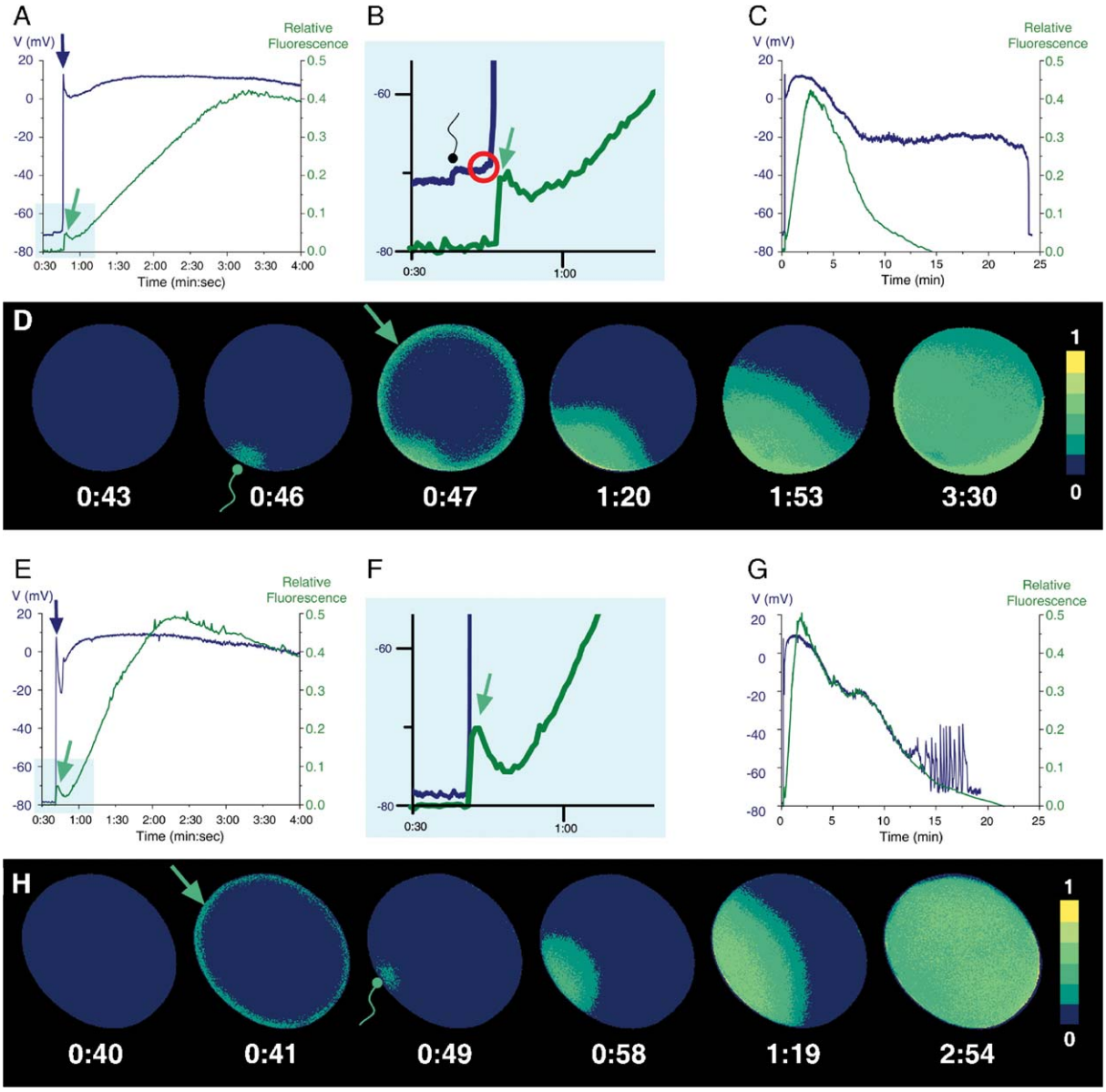

Fig. 2. Sperm-elicited FP and Ca^{2+} wave in *A. auranciacus* oocytes. The onset of the membrane depolarization and the concomitant Ca^{2+} signal in two different inseminated oocytes are shown as functions of time (blue and green traces, respectively) in panels A and E. (B and F) Expanded sections of the traces in panels A and E to highlight the presence (B) or the absence (F) of the step before the AP. The "pacemaker" depolarization which leads to the triggering of the regenerative process in panel B is enclosed within a red circle. (C and G) Complete time course of the responses shown in panels A and E. (D and H) Sequence of the relative fluorescence images illustrating the onset and the propagation of the sperm-induced Ca^{2+} wave in starfish oocytes where the Ca^{2+} spot precedes (D) or follows (H) the cortical flash. In this and the following figures, the occurrence of both the step and the spot is marked by a sperm symbol, while the sperm has been added at 30 s. Note that the green Ca^{2+} trace in panel C declines to the baseline before the membrane repolarization. It is likely that submembranal level of Ca^{2+} falls below the resolution limit of our CCD camera and is not detected (see Moccia et al., 2003b). The blue potential trace in panel G shows a brief train of spikes towards the end of the response. Such a pattern has been observed in a small number of oocytes and is shown here as an example.

(n = 73) (blue traces in Figs. 2A and E). The FP lasted 27.9 ± 1.8 min (n = 55) (blue traces in Figs. 2C and G).

The profile of the intracellular Ca^{2+} signal did depend on the initial pattern of the FP. The Ca^{2+} spot preceded or followed the cortical flash produced by the Ca^{2+}-AP depending on whether or not the depolarizing step preceded the regenerative process. In the first group of cells, the Ca^{2+} spot followed the voltage step by 3.4 ± 0.2 s (n = 26) and was localized at the putative site of sperm entry (sperm symbol in Fig. 2D). The Ca^{2+} spot in turn preceded the "pacemaker" depolarization (red circle in Fig. 2B) and the following Ca^{2+} flash (green arrow in Fig. 2D) by 0.70 ± 0.13 s (n = 17) and 3.5 ± 0.5 s (n = 27), respectively. In contrast, in the second class of oocytes, the cortical flash (green arrow in Fig. 2H) preceded the Ca^{2+} spot (sperm symbol in Fig. 2H) by 2.9 ± 0.2 s (n = 41) which is not significantly different from the lag between the step and the spot (P = 0.171). Whatever the order between the Ca^{2+} spot and the flash may be, the initial Ca^{2+} increase propagated as a single-source wave to the antipode of the cells with a speed of 1.94 ± 0.10 μm/s (n = 30) (see the sequence of relative fluorescence images in Figs. 2D and H). The graph of the relative fluorescence of the Ca^{2+} dye offers a numerical equivalent of the pseudocolors in the whole oocyte (green traces in Figs. 2A–C and E–G). The cortical Ca^{2+} flash appeared as a transient deflection (green arrows in Figs. 2A–B and E–F) that preceded the main Ca^{2+} increase, peaked at 0.041 ± 0.002 a.u. (n = 71) and lasted 5–10 s. The global Ca^{2+} transient reached the maximum amplitude of 0.447 ± 0.009 a.u. (n = 67) at 117.8 ± 3.6 s after the spot (n = 70) (green traces in Figs. 2A and E). The kinetics of the Ca^{2+} elevation did not closely match the time course of the FP. The V_m attained the peak of the slow depolarization (blue traces in Figs. 2A and E) 49.7 ± 5.0 s (n = 66) before the peak of the Ca^{2+} increase (green traces in Figs. 2A and E), while the average duration of the Ca^{2+} transient was 24.6 ± 1.1 min (n = 61) (green traces in Figs. 2C and G), which is not significantly different from the length of the FP (P = 0.113) (blue traces in Figs. 2C and G).

Our previous study showed that NAADP may trigger the FP in starfish oocytes (Moccia et al., 2004). Therefore, the simultaneous measurement of Ca^{2+} images and V_m carried out in our present study provides the first functional evidence that NAADP likely is the first messenger recruited by the fertilizing sperm in starfish (see also Discussion). The different patterns of the response could be related to the lower R_{input} of mature oocytes that exhibited the depolarizing step before the AP. Indeed, the R_{input} of the cells where the Ca^{2+} spot preceded the cortical flash was 102.6 ± 9.5 MΩ (n = 14), which is significantly lower (P = 0.00361) than the value, 324.4 ± 39.2 MΩ (n = 48), measured in the oocytes where the cortical flash followed the Ca^{2+} spot. Hereafter, we will refer to these two classes of cells as to low R_{input} oocytes and high R_{input} oocytes. In the latter, the voltage response to sperm rapidly induces a large depolarization, which obscures the depolarizing step visible in low R_{input} oocytes (Dale and Santella, 1985; Lynn et al., 1988; McCulloh et al., 1987; Miyazaki and Hirai, 1979). It is noteworthy that cells falling into either group could be extracted from the same animal on the same day during the whole breeding season of *A. auranciacus*. The mechanism responsible for the difference in R_{input} between the two types of cells is unclear and certainly deserves further studies. However, it likely depends on the differential decrease in the inwardly rectifying K^+ current, which is the conductance regulating R_{input} in starfish oocytes (Miyazaki et al., 1975; Moody and Lansman, 1983).

Functional NAADP receptors are required for the onset of the Ca^{2+} wave at fertilization

In order to assess the involvement of NAADP-dependent Ca^{2+} entry in the onset of the intracellular Ca^{2+} wave, it was necessary to block the response to NAADP. A specific inhibitor of NAADP receptors is still unavailable, but we have previously reported that the NAADP-activated Ca^{2+} current is sensitive to the blocker of receptor-operated channels, SK&F 96365 (SK and F) (Lim et al., 2001; Moccia et al., 2003a). In the presence of SK&F (10 μM), sperm could not activate oocytes (n = 5; not shown). However, the interpretation of this observation requires caution since SK&F prevents the acrosomal reaction in sea urchin (Hirohashi and Vacquier, 2003). Therefore, we used ligand-based desensitization of NAADP receptors in which receptors are inactivated by sub-threshold doses of NAADP prior to their opening (Genazzani and Billington, 2002; Santella et al., 2005). Indeed, the desensitization of NAADP receptors has been widely exploited to investigate whether an array of agonist-evoked Ca^{2+} signals were mediated by NAADP (Cancela et al., 1999, 2000; Johnson and Misler, 2002; Moccia et al., 2004; Santella, 2005). Briefly, it has been proposed that NAADP receptors possess two binding sites for NAADP of high and low affinity. The high affinity site mediates channel inactivation, whereas the low affinity site mediates channel opening. At low concentrations of NAADP, the high affinity site will be preferentially occupied and the channel will tend to inactivate. Thus, subsequent challenge with a higher dose of NAADP will not mediate channel opening (Patel, 2004). In control oocytes, the photolysis of 1 μM NAADP stimulated an AP with a latency of 8.8 ± 3.1 s (n = 7) (blue trace in Fig. 3B). The regenerative process triggered at a threshold of −61.4 ± 2.5 mV (n = 7), attained a positive overshoot at +16.0 ± 4.9 mV (first blue arrow in Fig. 3B) and, in 3 out of 7 cells, rapidly returned to the baseline (blue trace in Fig. 3B). In the remaining 4 cells, the membrane potential decayed to a plateau level of −52.0 ± 2.0 mV for approximately 90 s before repolarizing (not shown). The regenerative process was always followed by 1 up to 16 additional action potentials, whose biophysical properties were not different from the first one (see, for instance, the second blue arrow in Fig. 3B). The duration of the bioelectric response to NAADP ranged from 1 to 38 min, averaging 16.9 ± 4.5 min (n = 7). Every Ca^{2+}-AP caused a cortical flash (green arrows in Fig. 3A), which peaked at 0.041 ± 0.006 a.u. (n = 7) (green arrows in Fig. 3B) and did not spread throughout the cytosol (see the sequence of relative fluorescence images in Fig. 3A). Notably, the raise in cortical

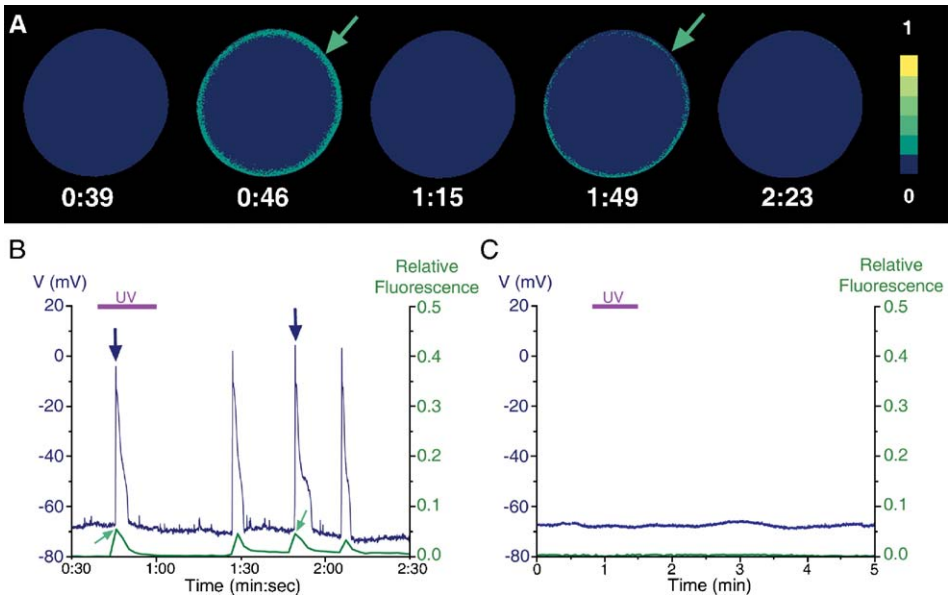

Fig. 3. The response to NAADP is desensitized by a subthreshold dose of the second messenger. (A) Repetitive Ca^{2+} flashes produced by the repetitive firing of Ca^{2+}-AP (blue arrows in panel B) which occurs upon NAADP (1 μM) uncaging in control starfish oocytes. Only the cortical flashes elicited by the first and the third AP are illustrated. Note that the cortical flashes fail to spread throughout the oocyte. (B) The blue trace tracks the periodic membrane depolarizations, while the green trace depicts the time course of the simultaneous Ca^{2+} signal. (C) The response to NAADP is absent in an oocyte preinjected with a sub-threshold dose (10 nM) of the agonist. The duration of UV flash is indicated by the horizontal purple bar.

Ca^{2+} level never preceded membrane depolarization upon uncaging of 1 μM NAADP. The photolysis of a lower concentration of NAADP (10 nM) did not elicit any Ca^{2+} signaling in starfish oocytes. However, the response to 1 μM NAADP was suppressed by preinjecting the sub-threshold concentration of the agonist (10 nM) 10 min before the uncaging (Fig. 3C). Therefore, in the subsequent experiments, we fertilized oocytes that had been previously desensitized to NAADP. In 7 out of 12 desensitized oocytes, the sperm did not induce either the FP or the Ca^{2+} wave (not shown). In the remaining 5 oocytes, the pattern of the ionic response to sperm was significantly altered, i.e., the Ca^{2+} elevation occurred prior to membrane depolarization. Indeed, the first detectable signal was a cortical Ca^{2+} spot (second relative fluorescence image in Fig. 4A), which was localized to the putative site of sperm entry and preceded by 4.5 ± 3.8 s (n = 5) a slow membrane depolarization that did not trigger a regenerative process in the oocyte shown in Fig. 4B (blue trace). That the Ca^{2+} level increased before the positive shift in V_m is clearly illustrated in Fig. 4C, which shows the onset of the response to the sperm at an expanded time scale. The second sperm fertilized the oocyte during the repolarizing phase, thus producing a second Ca^{2+} spot (third relative fluorescence image in Fig. 4A) which depolarized again the membrane and resulted in a cortical Ca^{2+} flash (green arrow in Fig. 4A). On average, the cortical flash followed by 22.3 ± 14.3 s (n = 5) the initial Ca^{2+} increase in NAADP-desensitized oocytes. The amplitudes of the Ca^{2+}-AP (blue arrow in Fig. 4B) and the cortical flash (green arrow in Fig. 4B) were slightly lower than in control cells (Fig. 4C), but the difference was not significant (Table 1). When the Ca^{2+} wavefronts coalesced, they produced a Ca^{2+} transient whose peak and kinetics were similar to those recorded in uninjected oocytes (Fig. 4B and Table 1B). The membrane potential, in turn, underwent a slower positive shift (blue trace in Fig. 4B), which reached a lower value (P = 0.015) than in control oocytes 64.1 ± 23.7 s (n = 5) before the Ca^{2+} peak (green trace in Fig. 4B; Table 1A). The intracellular Ca^{2+} level and V_m returned to the baseline within 30 min both in desensitized and uninjected cells (Table 1).

Hence, these results clearly indicate that starfish oocytes require functional NAADP receptors not only to trigger the FP upon sperm binding, but also to initiate the intracellular Ca^{2+} wave under physiological conditions.

The $InsP_3$ signaling boosts the "pacemaker" depolarization and prolongs the FP by activating a Ca^{2+}-dependent Na^+ entry

In our previous report (Moccia et al., 2004), we suggested that Ca^{2+} release from $InsP_3Rs$ maintained the membrane depolarization induced by NAADP at fertilization, but we did not investigate this issue in detail. Therefore, in the next set of experiments, we pre-injected mature oocytes with heparin (500 μg/ml), which competes with $InsP_3$ for binding sites on $InsP_3Rs$ (Ghosh et al., 1988). As expected, heparin did not prevent the firing of the Ca^{2+}-AP (blue trace in Fig. 5B and Table 1A), which could be either preceded by the depolarizing step (sperm symbol in Fig. 5C) or not (data not shown), depending on R_{input}. The peaks of both the depolarizing step and the AP were insensitive to heparin (Table 1A). The delay between the membrane depolarization and the Ca^{2+} spot was also unaffected (Table 1A). Surprisingly, in low R_{input} cells, we observed large variability in the time elapsing between the Ca^{2+} spot and the cortical flash, which was likely due to irregular intervals from the Ca^{2+} spot and the "pacemaker" depolarization (Table 1B). Consistently with previous studies

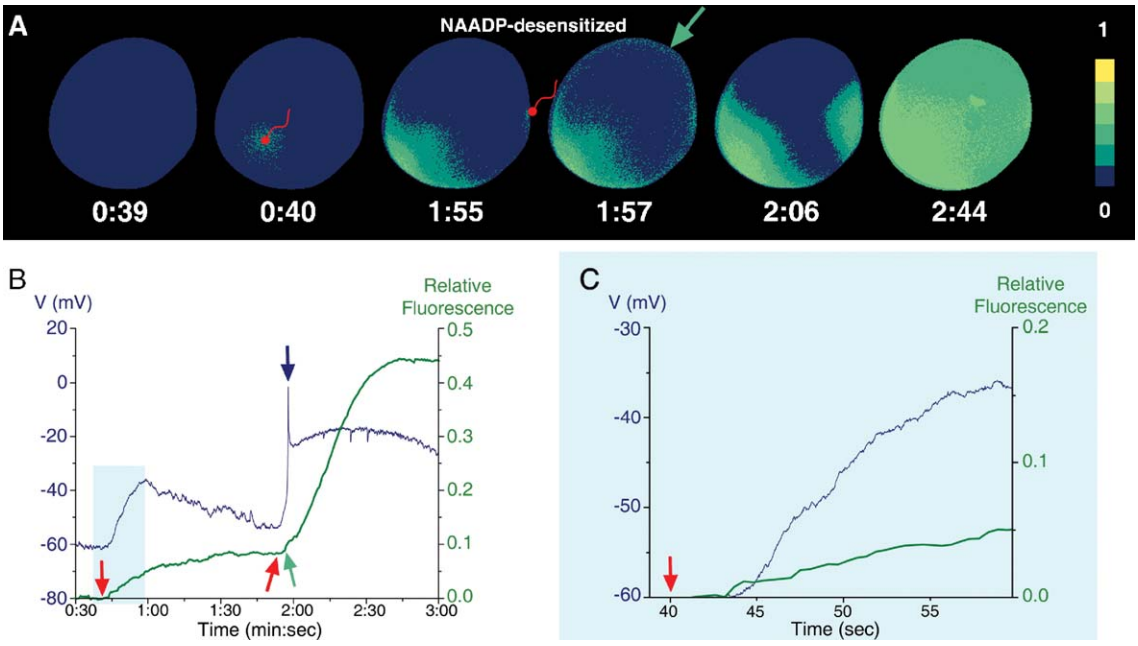

Fig. 4. The desensitization of NAADP receptors alters the pattern of the response at fertilization. (A) Sequence of the relative fluorescence images illustrating the pattern of the intracellular Ca^{2+} increase in an oocyte inseminated after preinjection with a sub-threshold dose (10 nM) of NAADP. This oocyte was fertilized by two sperms, which produced two Ca^{2+} wavefronts spreading to the entire cytoplasm. The red sperm symbols indicate the Ca^{2+} spots elicited by the two sperms at the beginning of the two Ca^{2+} waves. Note that the first Ca^{2+}spot (second relative fluorescence image) is slightly out of focus since the sperm binds to the upper surface of the oocyte: this is why it appears broader than in the other experiments shown in the manuscript. However, the second Ca^{2+} spot produced by the binding of a second sperm (third relative fluorescence image) is clearly on focus and displays an evident cortical location. (B) The green trace tracks the Ca^{2+} increase in the oocyte shown in panel A, while the blue trace shows the accompanying membrane depolarization. The two red arrows mark the time of appearance of the two Ca^{2+} spots on the Ca^{2+} trace. (C) The same as in panel B at an expanded time scale to show that the Ca^{2+} signal (indicated by the red arrow) precedes the positive shift in V_m.

(Stricker, 1995), the Ca^{2+} spot failed to propagate as a full-blown wave (see relative fluorescence images in Fig. 5A), thus resulting in a smaller and shorter Ca^{2+} elevation (green trace in Fig. 5B and Table 1B). The abolishment of the Ca^{2+} wave resulted in the suppression of the slow depolarization that followed the AP in oocytes with functional $InsP_3Rs$ (blue trace in Fig. 5B and Table 1A). Therefore, the membrane potential decayed to the baseline earlier than in control cells (compare the blue traces in Figs. 5B and D; Table 1A). These results were confirmed by inhibiting $InsP_3$ synthesis with U73122 (10 μM) (Fig. 6 and Table 1A–B), a blocker of phospholipase C (PLC), the enzyme which cleaves $InsP_3$ from phosphatidylinositol 4,5-bisphosphate (PIP_2). Importantly, the inactive analogue, U73343 (10 μM), did not affect the response to sperm (not shown). U73122 may exert pleiotropic effects on other cellular functions, such as inhibiting the internal Ca^{2+} pump, attenuating the $InsP_3$-depending Ca^{2+} release and blocking the cADPr/RyRs-dependent pathway (see Introduction in Lee et al., 1998). Control experiments, however, demonstrated that incubation with U73122 neither increased the basal Ca^{2+} level (n = 10; data not shown) nor affected the response to $InsP_3$ uncaging in starfish oocytes (n = 10; data not shown). As to the RyRs-mediated pathway, it does not seem to be involved in the ionic signaling induced by starfish sperm (see below). As previously reported (Santella et al., 1999), the rate of polyspermy was enhanced by 11% and 40%, respectively, in the cells injected with heparin or exposed to U73122. These oocytes could display multiple local Ca^{2+} increases (not shown), which were correlated with multiple sperm entry sites, either before or after the cortical flash. Moreover, the suppression of the $InsP_3$ pathway resulted in an abortive elevation of the fertilization envelope only at the site(s) where Ca^{2+} release occurred (Santella et al., 1999).

Collectively, these data provide the first evidence that the lag time between Ca^{2+} spot and cortical flash may be influenced by $InsP_3Rs$ and confirm the shortening of FP upon suppression of $InsP_3$ signaling (see also Moccia et al., 2004). Therefore, $InsP_3Rs$ may contribute to NAADP-induced depolarization upon sperm binding in starfish oocytes.

We have previously shown that Ca^{2+} release from $InsP_3Rs$ activated a Ca^{2+}-sensitive non-selective cation current that was sensitive to the removal of extracellular Na^+ (Moccia et al., 2003b). Hence, we have inseminated the oocytes after replacing extracellular Na^+ with an equimolar amount of choline. The first remarkable result was that Na^+ removal hyperpolarized the resting V_m from −28.2 ± 7.3 mV (n = 12) to −46.6 ± 5.4 mV (n = 17) and decreased R_{input} from 285.8 ± 70.3 MΩ to 98.8 ± 14.6 MΩ (n = 12). The negative shift in the resting potential upon Na^+ substitution has been already described in starfish and is likely due to the increase in Na^+ permeability during the maturation process (Miyazaki et al., 1975; Moccia et al., 2004). The drop in R_{input} is still unclear, but is probably linked to the changes in the membrane properties that occur during the resumption of the cell cycle. The low value of R_{input} in Na^+-FreeSW resulted in a step-like depolarization before the AP (first sperm

Table 1
Parameters of the FP (A) and the Ca^{2+} wave (B) elicited by the sperm in oocytes from *A. auranciacus*

A	V_c	Step	Lag between step and spot	Lag between step and AP	Upstroke	Well	Slow depolarization	Time to peak of slow depolarization	Duration
	(mV)	(mV)	(s)	(s)	(mV)	(mV)	(mV)	(s)	(min)
Control	−70.3 ± 1.6 (15)	3.1 ± 0.7 (5)	4.0 ± 0.4 (5)	7.9 ± 1.5 (5)	4.0 ± 4.5 (15)	−14.2 ± 4.9 (15)	14.7 ± 2.0 (13)	71.5 ± 6.4 (13)	**33.6 ± 1.8 (15)**
Heparin	−69.0 ± 1.2 (15)	3.7 ± 1.9 (11)	3.8 ± 0.7 (10)	62.9 ± 37.6 (11)	13.2 ± 3.2 (15)	Absent	Absent	Absent	**6.9 ± 1.8 (15)**
Control	−71.7 ± 1.4 (11)	5.2 ± 1.5 (5)	3.5 ± 0.9 (4)	5.5 ± 1.7 (4)	6.5 ± 4.0 (11)	−21.9 ± 5.1 (11)	11.5 ± 2.5 (10)	85.7 ± 1.5 (10)	**21.9 ± 0.9 (8)**
U73122	−69.5 ± 1.5 (12)	3.9 ± 0.9 (7)	4.6 ± 2.9 (5)	19.7 ± 13.9 (5)	−4.6 ± 4.7 (14)	Absent	Absent	Absent	**0.87 ± 0.38 (10)**
Control	−76.3 ± 1.9 (18)	4.1 ± 1.5 (5)	3.3 ± 0.6 (5)	6.1 ± 0.8 (5)	16.1 ± 4.4 (18)	−23.8 ± 4.8 (18)	8.0 ± 2.5 (18)	81.6 ± 8.7 (18)	28.8 ± 3.5 (16)
8-NH2-cADPr	−74.6 ± 2.0 (11)	3.4 ± 1.0 (5)	3.0 ± 1.2 (5)	4.9 ± 1.5 (5)	16.1 ± 5.2 (11)	−26.9 ± 3.4 (11)	4.9 ± 2.2 (11)	81.6 ± 14.5 (11)	23.0 ± 3.5 (9)
Ryanodine	−72.6 ± 3.6 (6)	3.1 ± 0.5 (3)	2.3 ± 0.6 (3)	4.6 ± 1.5 (3)	18.4 ± 4.7 (6)	−17.2 ± 11.1 (6)	15.8 ± 4.1 (6)	92.3 ± 9.6 (6)	26.8 ± 1.7 (4)
Ruthenium Red	−76.9 ± 3.9 (5)	NM	NM	NM	16.1 ± 6.0 (5)	−23.5 ± 4.2 (5)	8.3 ± 3.8 (5)	74.9 ± 6.3 (5)	26.3 ± 7.6 (3)
Control	−72.6 ± 1.8 (12)	2.8 ± 0.8 (4)	3.1 ± 0.5 (3)	**5.5 ± 1.5 (4)**	15.0 ± 1.4 (12)	−16.4 ± 3.2 (12)	**14.4 ± 1.9 (12)**	75.2 ± 8.7 (12)	**28.6 ± 5.2 (8)**
Na+-FreeSW	−71.4 ± 1.3 (17)	2.0 ± 0.3 (17)	3.8 ± 1.6 (9)	**16.1 ± 2.9 (9)**	11.5 ± 1.5 (14)	−12.0 ± 5.3 (14)	**−5.5 ± 2.7 (14)**	51.0 ± 10.1 (14)	**5.0 ± 0.8 (12)**
Control	−72.0 ± 1.7 (8)	3.9 ± 1.1 (5)	4.1 ± 0.5 (5)	9.0 ± 1.5 (5)	18.6 ± 3.7 (8)	**−13.9 ± 4.8 (8)**	**6.7 ± 4.9 (8)**	77.1 ± 11.4 (8)	24.8 ± 2.3 (4)
NAADP	−73.6 ± 2.3 (12)	Absent	Absent	Absent	3.1 ± 9.1 (5)	**−40.6 ± 11.4 (5)**	**−16.5 ± 6.5 (5)**	47.6 ± 17.6 (5)	22.3 ± 4.5 (5)

B	Lag between spot and "pd"	Lag between spot and flash	Flash Peak	Lag between flash and spot	Time to peak o f the wave	Wave Peak	Wave Speed	Duration
	(s)	(s)	(a.u.)	(s)	(s)	(a.u.)	(μm/s)	(min)
Control	1.2 ± 0.3 (5)	3.7 ± 1.4 (5)	0.033 ± 0.005 (15)	2.8 ± 0.2 (6)	120.7 ± 11.4 (14)	**0.42 ± 0.01 (15)**	2.3 ± 0.3 (7)	**27.1 ± 2.2 (12)**
Heparin	55.1 ± 42.4 (10)	57.7 ± 36.9 (10)	0.045 ± 0.013 (15)	3.5 ± 1.9 (4)	Absent	**0.12 ± 0.10 (12)**	Absent	**9.9 ± 1.8 (11)**
Control	0.56 ± 0.43 (4)	3.7 ± 1.2 (4)	0.042 ± 0.005 (11)	3.5 ± 0.6 (6)	117.2 ± 6.5 (11)	**0.46 ± 0.02 (11)**	2.0 ± 0.2 (6)	**25.6 ± 2.3 (9)**
U73122	12.5 ± 9.6 (5)	14.4 ± 10.2 (5)	0.032 ± 0.005 (12)	3.9 ± 2.9 (5)	Absent	**0.05 ± 0.02 (7)**	Absent	**1.1 ± 0.5 (7)**
Control	0.43 ± 0.21 (5)	3.2 ± 0.4 (5)	0.042 ± 0.004 (18)	3.5 ± 0.4 (12)	124.7 ± 8.9 (18)	0.45 ± 0.02 (18)	1.9 ± 0.2 (7)	24.4 ± 2.1 (18)
8-NH2-cADPr	0.58 ± 0.38 (5)	2.0 ± 1.6 (5)	0.032 ± 0.005 (11)	3.1 ± 0.7 (5)	115.1 ± 8.3 (11)	0.49 ± 0.03 (11)	1.31 ± 0.02 (4)	21.4 ± 2.6 (10)
Ryanodine	0.4 ± 0.31 (3)	1.8 ± 1.1 (3)	0.035 ± 0.005 (6)	3.6 ± 0.3 (3)	112.3 ± 3.1 (6)	0.43 ± 0.02 (6)	1.94 ± 0.08 (3)	23.0 ± 1.1 (5)
Ruthenium Red	NM	NM	0.0478 ± 0.0003 (5)	2.6 ± 0.3 (5)	105.9 ± 11.1 (5)	0.47 ± 0.01 (5)	1.92 ± 0.06 (3)	26.8 ± 4.3 (4)
Control	0.40 ± 0.09 (3)	2.2 ± 0.2 (3)	0.038 ± 0.007 (10)	1.9 ± 0.2 (8)	98.8 ± 7.5 (10)	0.48 ± 0.03 (10)	1.7 ± 0.1 (5)	20.8 ± 1.4 (10)
Na+-FreeSW	4.5 ± 1.9 (9)	12.1 ± 3.0 (9)	0.051 ± 0.006 (17)	Absent	91.5 ± 5.7 (15)	0.43 ± 0.03 (15)	2.6 ± 0.5 (5)	21.8 ± 2.5 (13)
Control	0.89 ± 0.02 (5)	4.5 ± 1.4 (5)	0.044 ± 0.010 (8)	Only 1 cell	116.3 ± 9.7 (8)	0.42 ± 0.03 (8)	1.7 ± 0.4 (4)	27.9 ± 3.4 (6)
NAADP	See text	See text	0.020 ± 0.088 (5)	Absent	110.7 ± 2.4 (5)	0.42 ± 0.02 (5)	Not measurable	28.2 ± 1.2 (3)

Each value represents the average ± SE of 4–10 cells. In each column, values marked in bold are significantly different. The experiments were performed by recording on the same day from the same number of control oocytes and pharmacologically treated cells. Pd is the abbreviation for "pacemaker" depolarization.

Parameters of the FP (A) and the Ca^{2+} wave (B) elicited by sperm in starfish oocytes. In each column, values marked in bold are significantly different. The number of cells analyzed for each condition is indicated in parentheses. The experiments were performed by recording on the same day from the same number of control oocytes and pharmacologically treated cells. Pd is the abbreviation for "pacemaker" depolarization. Note that the animals that we used for the experiments with ruthenium red provided only high R_{input} oocytes both under control conditions and after drug injection.

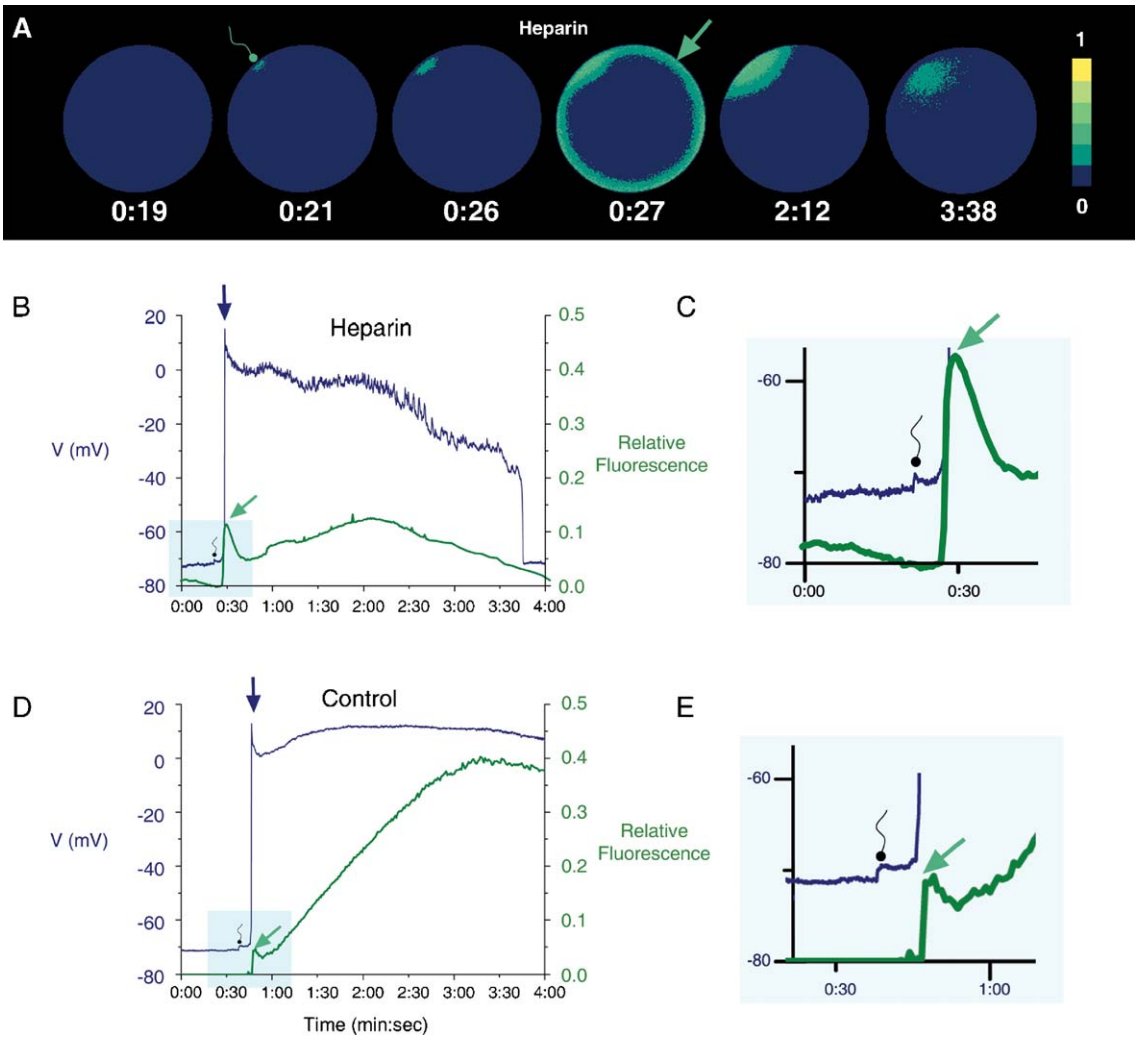

Fig. 5. Heparin impairs the propagation of the sperm-induced Ca^{2+} wave, but not the onset of the FP. (A) Sequence of the relative fluorescence images illustrating the pattern of the intracellular Ca^{2+} increase in an oocyte preinjected with heparin (500 μg/ml). The Ca^{2+} spot does not propagate farther than the site of sperm fusion after inhibition of $InsP_3Rs$. (B) The onset of the FP and the Ca^{2+} elevation measured in the oocyte shown in panel A are tracked by the blue and green traces, respectively. (C) An extended section of the traces in B to highlight the step and the "pacemaker" depolarization before the AP. (D) Beginning of the FP (blue trace) and of the Ca^{2+} increase (green trace) in a control oocyte. (E) The same as in panel D at an expanded time scale. Note the shorter duration of the response and the lower amplitude of the Ca^{2+} elevation in the heparin-treated oocyte.

symbol in Fig. 7C). Although the latency between the step and the Ca^{2+} spot (sperm symbol in Fig. 7A) was unaffected by Na^+ replacement (Table 1A), we observed a large heterogeneity in the time elapsing between the spot and the "pacemaker" depolarization (Table 1B). This feature, in turn, caused a large variability in the delay between the Ca^{2+} spot and cortical flash (second to fourth relative fluorescence image in Fig. 7A; Table 1B) and could enhance the rate of polyspermy in Na^+-FreeSW (17.6% vs. 0.0 in ASW) (second sperm symbol in Fig. 7C). The slower depolarization after the rapid AP in Na^+-FreeSW either attained a smaller level than in NSW (n = 12) (blue traces in Figs. 7C and E; Table 1A) or even disappeared (n = 5). The FP was, therefore, significantly shortened upon Na^+ replacement (compare blue traces in Figs. 7B and D; Table 1A). Importantly, neither the peak nor the kinetics of the Ca^{2+} wave were affected under these conditions (Table 1B).

Altogether, these data demonstrate that Na^+ entry sustains the membrane depolarization initiated by NAADP at fertilization. Na^+ inflow is likely mediated by the Ca^{2+}-sensitive cation conductance activated upon Ca^{2+} release from the $InsP_3Rs$ (Moccia et al., 2003b; see also below). Moreover, in low R_{input} cells, the Ca^{2+}-mediated Na^+ influx boosts the "pacemaker" depolarization that precedes the regenerative process (see Discussion).

cADPr and RyRs do not participate to the Ca^{2+} signaling at fertilization

The involvement of cADPr/RyRs in the sperm-induced response is still debated in starfish (Nusco et al., 2002). This issue was investigated by first injecting the oocytes with 8-NH_2-cADPr (4 μM) (Lee et al., 1993), which was previously shown to hinder the cADPr-sensitive Ca^{2+} release in these cells

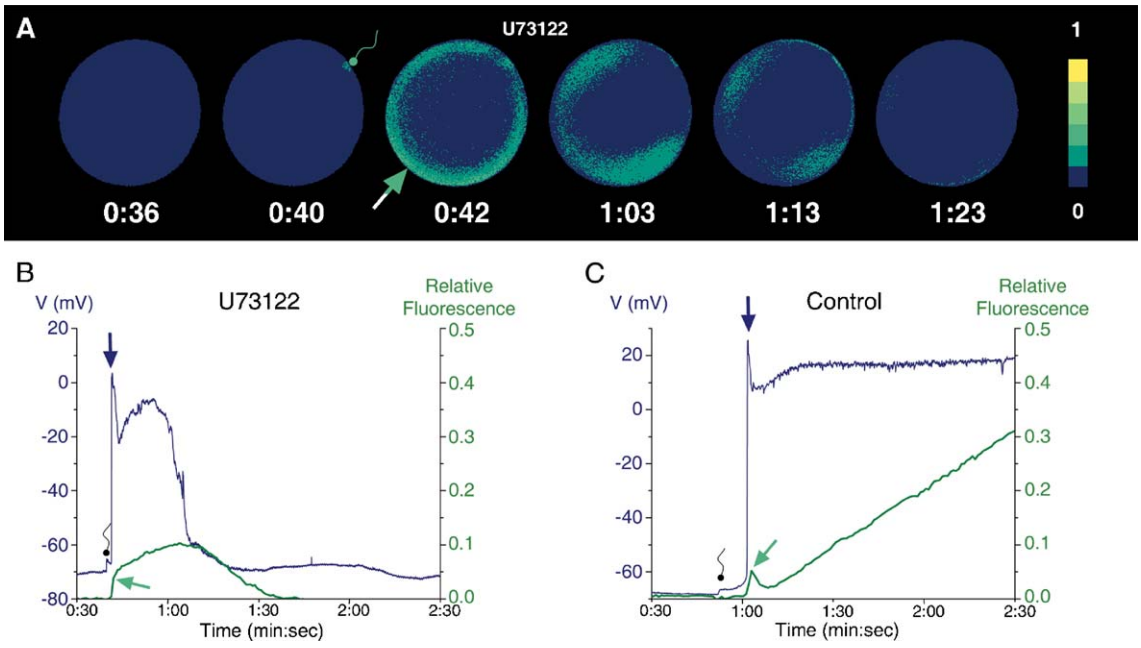

Fig. 6. U73122 affects the spreading of the sperm-elicited Ca^{2+} wave, but not the onset of the FP. (A) Sequence of the relative fluorescence images illustrating the pattern of the intracellular Ca^{2+} increase in an oocyte preincubated in 10 μM U73122 before insemination. The Ca^{2+} spot fails to spread toward the antipode of the oocyte upon inhibition of PLC. (B) The onset of the FP and the Ca^{2+} elevation which occur in the oocyte shown in panel A are tracked by the blue and green traces, respectively. (C) Beginning of the FP (blue trace) and of the Ca^{2+} increase (green trace) in a control oocyte. Note the shorter duration of the response and the lower peak of the Ca^{2+} transient in the U73122-treated oocyte.

(Moccia et al., 2003b). The pre-treatment with 8-NH_2-cADPr neither prevented nor attenuated the ionic response to sperm (Fig. 8C and Table 1A–B), although it caused an increase in the rate of polyspermy (91% vs. 0% in control oocytes), which resulted in the occurrence of more steps and Ca^{2+} spots during the early phase of the FP (see the sperm symbols in Fig. 8C). When additional sperms bound the membrane after the Ca^{2+}-AP (first blue arrow in Fig. 8C), they produced additional Ca^{2+} spikes (second blue arrow in Fig. 8C). However, the fertilization envelope elevated normally in these cells (not shown). We injected another antagonist of cADPr, 8-Br-cADPr, but it activated the oocytes, which thus could not be inseminated (not shown).

In order to test the role of RyRs, we injected into the cytosol either ruthenium red (20 μM) (not shown) or ryanodine (200 μM) (Fig. 8B), two known blockers of RyRs (Gerasimenko and Gerasimenko, 2005). Control experiments showed that the two inhibitors either damped or suppressed the Ca^{2+} oscillations induced by the RyRs agonist caffeine (5 mM) in starfish oocytes (n = 5 for ruthenium red and n = 8 for ryanodine; unpublished results). However, they did not impair either the FP or the Ca^{2+} wave (Table 1A–B), nor augmented the rate of polyspermy.

These data suggest that the cADPr/RyRs-dependent pathway does not play any evident role in the ionic response to sperm. It remains to clarify whether cADPr contributes to the fast block to polyspermy through a mechanism unrelated to RyRs activation or whether 8-NH_2-cADPr makes starfish oocytes more prone to polyspermy due to a yet unknown side effect. This investigation, however, was beyond the aim of the present study.

The uncaging of $InsP_3$ produces a Ca^{2+} wave that precedes the membrane depolarization

The anomalous pattern of the response to sperm in NAADP-desensitized oocytes was likely due to the activation of the $InsP_3$Rs, as the RyRs were ruled out by the experiments described above. We investigated this issue by photoliberating a saturating concentration of caged $InsP_3$ (100 nM) (Lim et al., 2003). $InsP_3$ ignited an intracellular Ca^{2+} release, which was initially restricted to the cortical region of the oocyte (red arrow in Fig. 9A) and started after a latency of 5.6 ± 1.0 s, which is similar to the delay we have previously reported (Lim et al., 2001). The Ca^{2+} elevation preceded a membrane depolarization by 8.4 ± 4.4 s (n = 13) (Fig. 9C). When V_m attained a threshold of − 65.3 ± 3.4 mV (n = 10), a Ca^{2+}-AP triggered, which peaked at +1.2 ± 5.4 mV (n = 11) (blue trace in Fig. 9B) and produced a cortical flash (green arrow in Fig. 9A) that spread inwardly to the centre (see the last three relative fluorescence images in Fig. 9A). The global Ca^{2+} increase reached a peak of 0.62 ± 0.04 a.u. (n = 14) at 25.2 ± 2.6 s after the first elevation (green trace in Fig. 9B), while V_m decayed to a plateau level of −3.1 ± 5.6 mV (n = 12) (blue trace in Fig. 9B). The $InsP_3$-evoked Ca^{2+} explosion resulted in the elevation of the fertilization membrane (not shown). The Ca^{2+} level and the membrane potential returned to the baseline after 477.3 ± 69.4 s (n = 7) and 360.0 ± 131.8 s (n = 13), respectively. The positive shift in V_m caused by $InsP_3$ was likely due to the activation of a Ca^{2+}-sensitive cation current (Moccia et al., 2003b). Accordingly, neither the Ca^{2+} release nor the membrane depolarization occurred in oocytes pre-injected with heparin (500 μg/ml) (data not shown). These results show that the pattern of the response

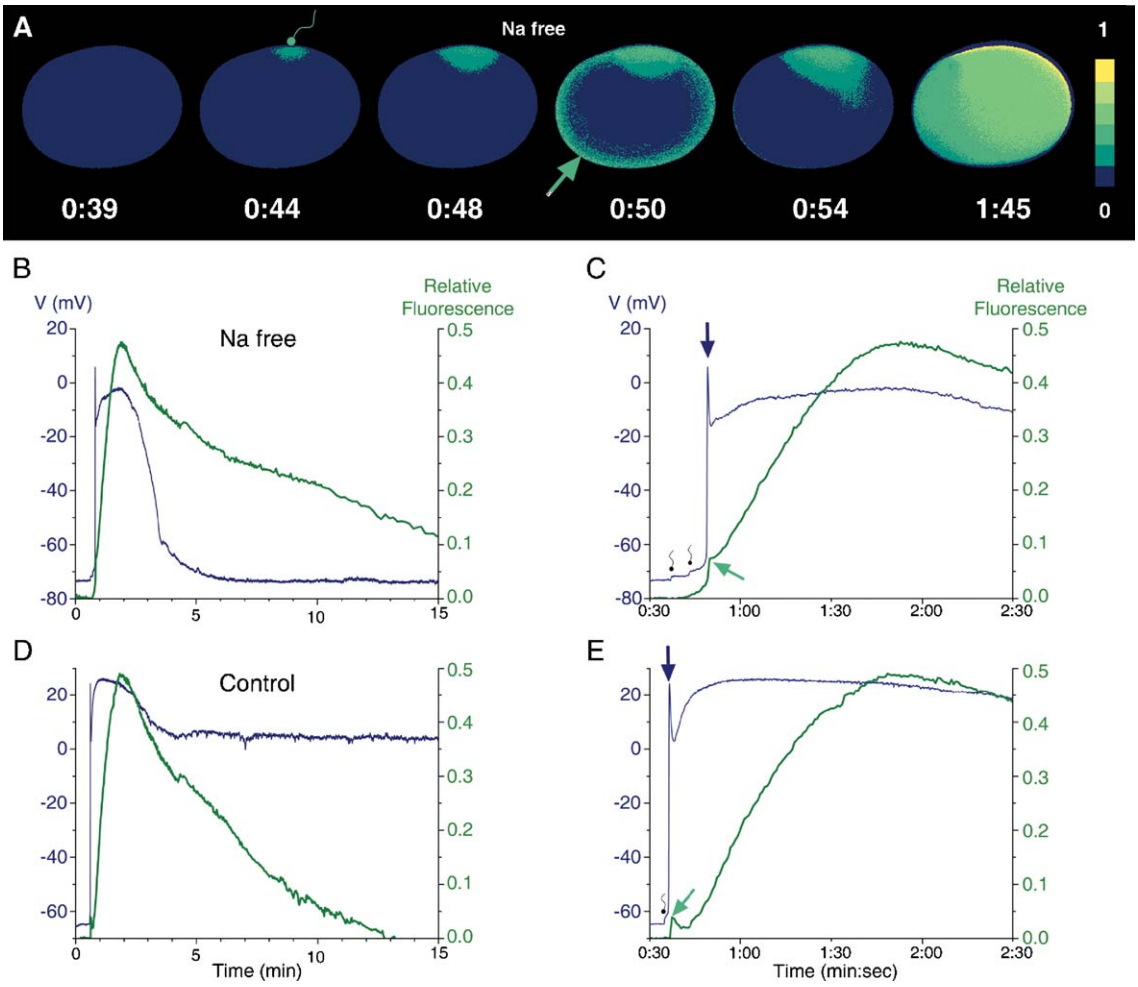

Fig. 7. Na^+ influx sustains the membrane depolarization at fertilization. (A) Sequence of the relative fluorescence images illustrating the onset and the propagation of the sperm-induced Ca^{2+} wave in Na^+-FreeSW. Note the longer time elapsing between the Ca^{2+} spot and the cortical flash as compared to an oocyte inseminated in ASW (see Fig. 2D). (B) The blue trace track the FP which occurs in the oocyte shown in panel A, while the green trace depicts the time course of the concomitant Ca^{2+} wave. (C) Extended section of the traces in panel B. The polyspermy in Na^+-FreeSW is highlighted by the two steps on the blue trace in panel C (each one marked by a sperm symbol). The Ca^{2+} spot associated to the second sperm is out of focus and is not displayed in panel A. (D) Time courses of the FP (blue trace) and of the intracellular Ca^{2+} increase (green trace) in a control oocyte. (E) The same as in D at an expanded time scale. Note the shorter duration of FP in Na^+-FreeSW.

to $InsP_3$ is similar to that observed at fertilization after the desensitization of NAADP receptors, i.e., the Ca^{2+} wave precedes the membrane depolarization.

Discussion

This study provides the first evidence that NAADP receptors are involved in the onset of the Ca^{2+} wave at the fertilization of starfish oocytes. Previous work from our laboratory had only focused on the role of NAADP as a trigger of the FP (Moccia et al., 2004). The data in this communication show that the Ca^{2+} wave promoted by $InsP_3$ is either absent or significantly modified upon desensitization of NAADP receptors. Ca^{2+} mobilization from $InsP_3$Rs, in turn, may foster NAADP-induced depolarization, a feature which underlines the complexity of the interplay between NAADP receptors and $InsP_3$Rs in the activation of echinoderm oocytes (Billington et al., 2002; Churchill et al., 2003; Moccia et al., 2004).

The pattern of initial Ca^{2+} signal at fertilization may vary within starfish species. The cortical Ca^{2+} flash, which is produced by Ca^{2+} influx during the Ca^{2+}-AP, may precede the Ca^{2+} wave in *A. miniata* oocytes (Carroll et al., 1997) and in approximately the 40% of *A. auranciacus* oocytes (Nusco et al., 2002; Fig. 2 of the present study), but the order of the events is inverted in the remaining 60% of the latter species. Moreover, as no evident Ca^{2+} flash is seen in *Pisaster ochraceous* oocytes, no temporal relationship can be established between membrane depolarization and intracellular Ca^{2+} release in this species (Stricker et al., 1994). The simultaneous imaging of the Ca^{2+} level and recording of V_m, described here has permitted the discovery that an abrupt depolarizing step before the Ca^{2+} spot appears even when the latter precedes the cortical flash. Since NAADP may trigger the FP in starfish oocytes, and the Ca^{2+} spot is the starting point for the intracellular wave (see below), it is conceivable that NAADP is the first Ca^{2+}-mobilizing messenger recruited at fertilization. The pattern of the response to sperm, in turn, seems to be related to oocyte R_{input}, as low R_{input} oocytes

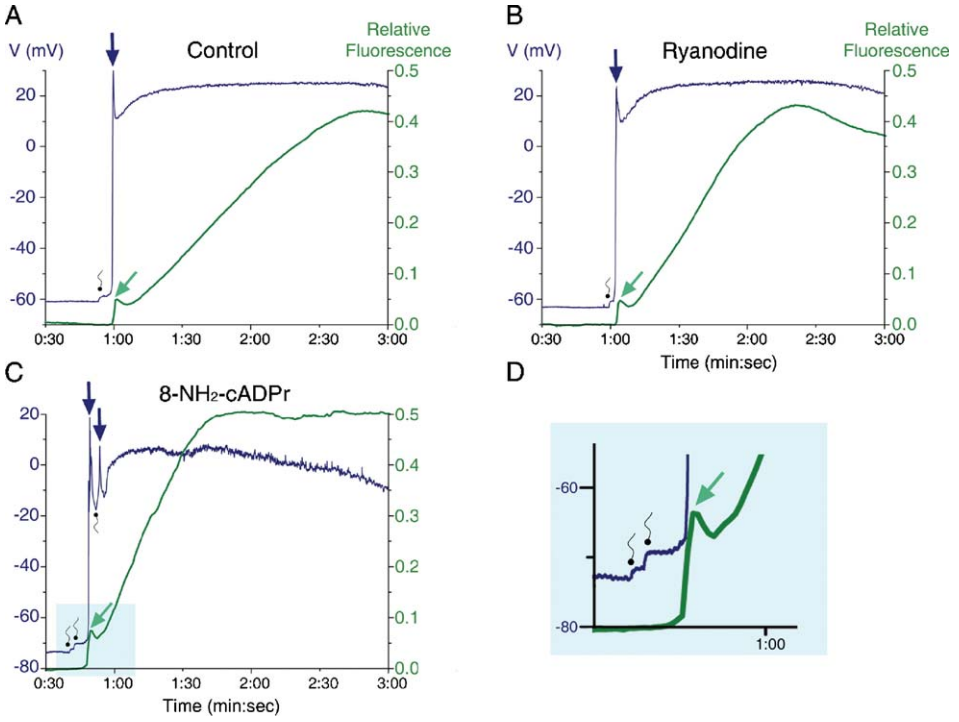

Fig. 8. cADPr and RyRs are not involved in the ionic signaling at fertilization. Onset of the voltage (blue traces) and Ca^{2+} (green traces) responses to the sperm in control (A), ryanodine-injected (200 μM) (B), and 8-NH_2-cADPr-injected oocytes (4 μM) (C). (D) The same as in panel C but at an extended time scale. The polyspermy in presence of 8-NH_2-cADPr is indicated by the sperm symbols which mark the occurrence of the steps in panels C and D and of a second AP in panel C.

display the Ca^{2+} spot before the cortical flash, while the order is inverted in high R_{input} cells. Possibly, when R_{input} is high, the initial voltage response to NAADP may directly trigger the regenerative process, which is then followed by the point source Ca^{2+} wave (McCulloh et al., 1987). Conversely, when R_{input} is low, NAADP may elicit a smaller potential change (the

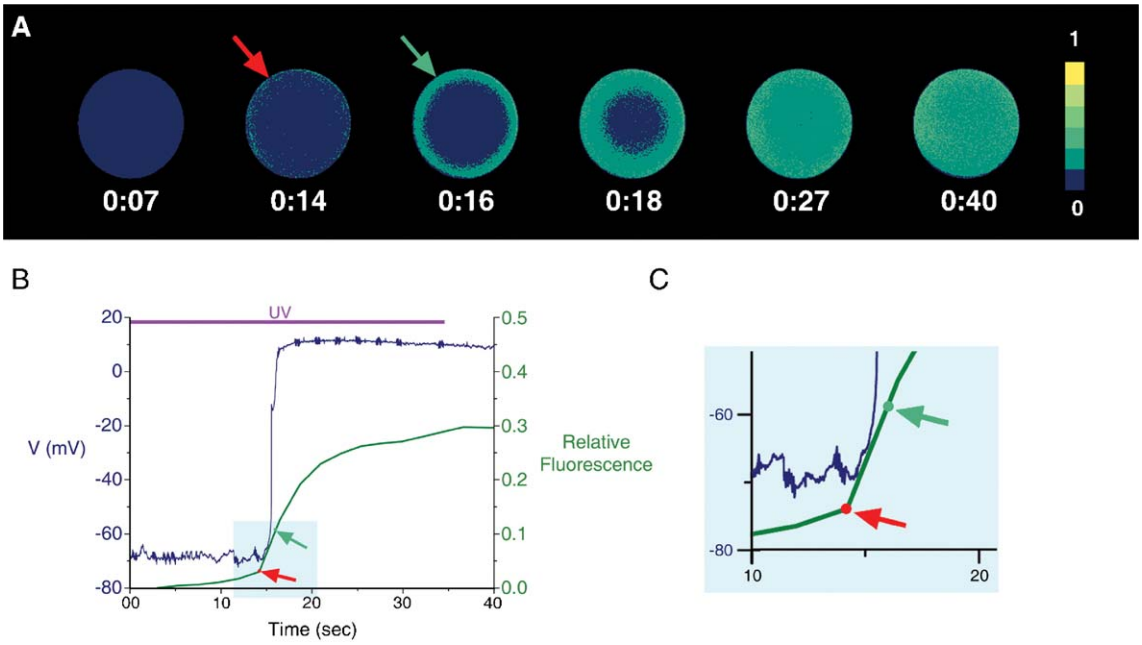

Fig. 9. The uncaging of $InsP_3$ elicits a Ca^{2+} increase followed by membrane depolarization. (A) Relative fluorescence images showing the onset and propagation of the Ca^{2+} wave upon photolysis of $InsP_3$ (100 nM). The red arrow marks the initial cortical Ca^{2+} response to $InsP_3$, while the green arrow indicates the cortical flash. (B) The green and blue traces track the onset of the Ca^{2+} elevation and of the following membrane depolarization, respectively. The duration of irradiation is indicated by the horizontal purple bar (the previous initial 10 s of the experiment have been cut). The red dot and the red arrow mark the initial Ca^{2+} response to $InsP_3$, while the green dot and the green arrow indicate the cortical flash. (C) Expanded section of the traces in panel B to highlight that the Ca^{2+} signal (red dot and red arrow) raises above the resting level before the change in V_m.

depolarizing step), associated to a cortical Ca^{2+} spot, which is followed by a slower depolarization (the "pacemaker" depolarization) to the threshold of activation of the voltage-gated Ca^{2+} channels (McCulloh et al., 1987). That the initial pattern of FP may be related to cell R_{input} is further supported by the observation that sea urchin sperm(s) evoke one or more depolarizing steps in the oocytes, but not in the eggs, which display a significantly higher R_{input} (Dale and Santella, 1985; Lynn et al., 1988; McCulloh et al., 1987). In addition, the pharmacological reduction of R_{input} in sea urchin eggs converts the initial fast (50–400 ms) depolarization to a step-like one, which then reaches the threshold of the Ca^{2+}-AP (Hülser and Schatten, 1982). Unfortunately, in these cells the concomitant Ca^{2+} wave has not been recorded.

That functional NAADP receptors play a key role in generating the sperm-induced Ca^{2+} wave in starfish oocytes is convincingly indicated by the lack of Ca^{2+} elevation in cells either pre-treated with the inhibitor SK&F or desensitized to NAADP. The abolishment of Ca^{2+} increase in oocytes desensitized to NAADP provides the first evidence that NAADP is involved in the initiation of the global Ca^{2+}. In sea urchin eggs pretreated with NAADP, the Ca^{2+} flash is also absent and the onset of the Ca^{2+} wave may be delayed (Churchill et al., 2003). These findings clearly pointed to the involvement of NAADP in the sperm-induced Ca^{2+} wave, but offered no clues on the nature of its triggering role since they are only based on the measurement of the Ca^{2+} level. As mentioned above, the simultaneous recording of Ca^{2+} images and V_m has shown that, even in the cells where the Ca^{2+} increase occurs, the pattern of the response is altered by the desensitization of NAADP receptors. Firstly, the Ca^{2+} elevation precedes by several seconds the membrane depolarization. Secondly, the cell is polyspermic probably due to the long time elapsing between the generation of the first spot and the Ca^{2+}-AP. The embryonic development of these oocytes is, therefore, predicted to be aberrant (Gould and Stephano, 2003). The anomalous response that may occur in some NAADP-desensitized oocytes further underscores the central role of NAADP in the onset of the Ca^{2+} wave under physiological conditions. Three pieces of evidence support the notion that $InsP_3$ is the only messenger underlying the response to sperm when NAADP receptors are desensitized. Firstly, the profile of activation is similar to that observed after $InsP_3$ uncaging in oocytes not challenged with the sperm: the Ca^{2+} release that follows $InsP_3$ uncaging would result in a cortical flash through the stimulation of the Ca^{2+}-sensitive Na^+ influx which depolarizes the membrane and activates the voltage-gated Ca^{2+} channels. Secondly, the peak of Ca^{2+} increase was not significantly different from that recorded under control conditions. Thirdly, the cADPr/RyRs-dependent pathway is not involved in the Ca^{2+} signaling at fertilization. Two mechanisms could explain the involvement of NAADP during the chain of events that leads to the beginning of the $InsP_3$-mediated Ca^{2+} wave (Stricker et al., 1994; Carroll et al., 1997; Lim et al., 2001; present experiments). The NAADP-dependent Ca^{2+} entry might contribute to the stimulation of PLCγ, the PLC isoform producing $InsP_3$ in starfish oocytes (Runft et al., 2004), which requires micromolar concentration of Ca^{2+} to be activated (Rhee, 2001). Alternatively, the inflow of Ca^{2+} caused by NAADP might sensitize the $InsP_3Rs$ at the site of sperm attachment through a process of Ca^{2+}-induced Ca^{2+} release (Alonso et al., 1999). The latency between the FP and the generation of the Ca^{2+} spot did not change whether the membrane depolarization consisted in either a step or action potential. This result suggests that the local accumulation of Ca^{2+} near the pores of the NAADP-activated channels was adequate for the initiation of the Ca^{2+} elevation.

The complex interplay between NAADP-receptors and $InsP_3Rs$ is further revealed by the large heterogeneity in the lag time between the depolarizing step and the AP either when the $InsP_3$-sensitive pathway is impaired or when extracellular Na^+ is removed. The extended delay between these two bioelectric events depends on the longer time elapsing between the Ca^{2+} spot and the "pacemaker" depolarization which fires the AP. In low R_{input} cells, the abrupt depolarization produced by NAADP fails to reach the threshold of activation of the voltage-gated Ca^{2+} channels. Our results strongly suggest that the $InsP_3$-dependent Ca^{2+} wave initiated after the step recruits the Ca^{2+}-activated cation channels to boost the membrane voltage to the threshold of the regenerative process. The "pacemaker" depolarization would thus be mainly sustained by a Ca^{2+}-elicited Na^+ entry. Na^+ influx is also necessary to maintain the membrane depolarization until the end of the response to sperm. Consistently, the membrane repolarizes earlier when the $InsP_3$ pathway has been blocked or when extracellular Na^+ has been replaced by choline.

As mentioned above, the Ca^{2+} spot detected after the initial depolarization is the starting point of the intracellular Ca^{2+} wave ignited by the sperm. The spot is likely to result from Ca^{2+} release from $InsP_3Rs$ (Stricker, 1995; Carroll et al., 1997). The occurrence of the spot even in cells in which the $InsP_3$ signaling is not functional does not imply that $InsP_3Rs$ do not mediate it. For instance, in cells injected with heparin, $InsP_3$ synthesis at the point of sperm attachment might be so high that heparin becomes displaced from their common binding site on the $InsP_3Rs$ (Ghosh et al., 1988). However, the contribution of the NAADP-dependent Ca^{2+} influx to the generation of the Ca^{2+} spot cannot be ruled out, as the accumulation of Ca^{2+} near the intracellular side of the pores of the NAADP-gated channels might contribute to it (Moccia et al., 2003a). Unfortunately, starfish oocytes cannot be fertilized in the absence of extracellular Ca^{2+}. Therefore, to definitively assess the nature and the source of Ca^{2+} spot, a different approach is required. We are currently undertaking a study to abrogate the PLCγ-dependent signaling by introducing an excess of the tandem SH2 domains into starfish oocytes (Runft et al., 2004). Interference of the endogenous PLCγ by this dominant mutant inhibitor may shed lights on this issue.

The evidence presented in this study strengthens the conclusion that NAADP may initiate the intracellular Ca^{2+} wave at fertilization in starfish oocytes. This is in line with the reported ability of NAADP to trigger a global Ca^{2+} signal from a specific sub-cellular region (Cancela et al., 2002, 2003; Churchill and Galione, 2001a). It is worth noting that NAADP has been suggested as a first actor in the initiation of the Ca^{2+}

signal in the two species displaying a single Ca^{2+} transient at fertilization, i.e., sea urchin (Churchill et al., 2003) and starfish (Lim et al., 2001 and present study). As the NAADP response appears to exhibit "a spatial memory of the previous response that shapes the spatial pattern of subsequent Ca^{2+} increases" (Churchill et al., 2002a,b), a spatially restricted increase in NAADP i.e., at the sperm binding site, would prevent the onset of another NAADP-dependent signal for a time (25 min) (Churchill and Galione, 2001b), corresponding to the duration of the Ca^{2+} elevation in echinoderms (Lee et al., 1993; present study). This feature, along with the restructuring of the ER during maturation (Santella et al., 2004), could explain the lack of repetitive Ca^{2+} increases in this *phylum*.

As to the requirement of extracellular Ca^{2+} in the NAADP-dependent response of starfish oocytes to sperm, it is appropriate to mention the work by Crèton and Jaffe (1995) in which the activation of sea urchin eggs was suppressed by preventing Ca^{2+} influx during the latent period between the Ca^{2+}-AP and the start of the Ca^{2+} wave. These authors attributed the Ca^{2+} explosion in eggs inseminated in Ca^{2+}-free seawater by an excess of reacted sperm to an unnatural mechanism (McDougall et al., 1993). They suggested that, under these conditions, Ca^{2+} was probably released from sperm mitochondria by the high extramitochondrial sodium concentration in acrosome-reacted sperm. These conclusions, therefore, nicely match the model of activation of starfish oocytes proposed here.

Acknowledgments

We thank Dr. F. Tanzi for critical reading of the manuscript, G. Gragnaniello for his valuable help in the preparation of the figures, J.T. Chun and E. Ercolano for the continuous scientific discussions. The help of the Marine Resource Service of the Stazione Zoologica for maintaining the starfish is also gratefully acknowledged.

References

Alonso, M.T., Barrero, M.J., Michelena, P., Carnicero, E., Cuchillo, I., Garcia, A.G., Garcia-Sancho, J., Montero, M., Alvarez, J., 1999. Ca^{2+}-induced Ca^{2+} release in chromaffin cells seen from inside the ER with targeted aequorin. J. Cell Biol. 144, 241–254.

Billington, R.A., Ho, R.A., Genazzani, A.A., 2002. NAADP is present at micromolar concentrations in sea urchin sperm. J. Physiol. 544, 107–112.

Cancela, J.M., 2001. Specific Ca^{2+} signaling evoked by cholecystokinin and acetylcholine: the roles of NAADP, cADPR, and IP_3. Annu. Rev. Physiol. 63, 99–117.

Cancela, J.M., Churchill, G.C., Galione, A., 1999. Coordination of agonist-induced Ca^{2+} signaling patterns by NAADP in pancreatic acinar cells. Nature 398, 74–76.

Cancela, J.M., Gerasimenko, O.V., Gerasimenko, J.V., Tepikin, A.V., Petersen, O.H., 2000. Two different but converging messenger pathways to intracellular Ca^{2+} release: the roles of nicotinic acid adenine dinucleotide phosphate, cyclic ADP-ribose and inositol trisphosphate. EMBO J. 19, 2549–2557.

Cancela, J.M., van Coppenolle, F., Galione, A., Tepikin, A.V., Petersen, O.H., 2002. Transformation of local Ca^{2+} spikes to global Ca^{2+} transients: the combinatorial roles of multiple Ca^{2+} releasing messengers. EMBO J. 21, 909–919.

Cancela, J.M., Charpentier, G., Petersen, O.H., 2003. Co-ordination of Ca^{2+} signalling in mammalian cells by the new Ca^{2+}-releasing messenger NAADP. Pfluegers Arch. 446, 322–327.

Carroll, D.J., Ramarao, C.S., Mehlmann, L.M., Roche, S., Terasaki, M., Jaffe, L. A., 1997. Calcium release at fertilization in starfish eggs is mediated by phospholipase Cγ. J. Cell Biol. 138, 1303–1311.

Churchill, G.C., Galione, A., 2001a. NAADP induces Ca^{2+} oscillations via a two-pool mechanism by priming IP3- and cADPr-sensitive Ca^{2+} stores. EMBO J. 20, 2666–2671.

Churchill, G.C., Galione, A., 2001b. Prolonged inactivation of nicotinic acid adenine dinucleotide phosphate-induced Ca^{2+} release mediates a spatiotemporal Ca^{2+} memory. J. Biol. Chem. 276, 11223–11225.

Churchill, G.C., et al., 2002a. NAADP mobilizes Ca^{2+} from reserve granules, a lysosome-related organelle, in sea urchin eggs. Cell 111, 73–708.

Churchill, G.C., Patel, S., Thomas, J.M., Galione, A., 2002b. Spatial and temporal control of calcium signaling by NAADP. In: Lee, K.W. (Ed.), Cyclic ADP-ribose and NAADP. Kluwer Academic Publishers, Dordrecht, pp. 199–215.

Churchill, G.C., O'Neill, J.S., Masgrau, R., Patel, S., Thomas, J.M., Genazzani, A.A., Galione, A., 2003. Sperm deliver a new second messenger: NAADP. Curr. Biol. 13, 247–251.

Crèton, R., Jaffe, L.F., 1995. Role of calcium influx during the latent period in sea urchin fertilization. Dev. Growth Differ. 37, 703–709.

Dale, B., Santella, L., 1985. Sperm-oocyte interaction in the sea urchin. J. Cell Sci. 74, 153–167.

Deguchi, R., Morisawa, M., 2003. External Ca^{2+} is predominantly used for cytoplasmic and nuclear Ca^{2+} increases in fertilized oocytes of the marine bivalve *Mactra chinensis*. J. Cell Sci. 116, 367–376.

Eckberg, W.R., Miller, A.L., 1995. Propagated and non propagated calcium transients during egg activation in the annelid, *Chaetopterus*. Dev. Biol. 172, 654–664.

Genazzani, A.A., Billington, R., 2002. NAADP: an atypical Ca^{2+} releasing messenger? Trends Pharmacol. Sci. 23, 165–167.

Gerasimenko, O., Gerasimenko, J., 2005. New aspects of nuclear calcium signalling. J. Cell Sci. 117, 3087–3094.

Ghosh, T.K., Eis, P.S., Mullaney, J.M., Ebert, C.L., Gill, D.L., 1988. Competitive, reversible, and potent antagonism of inositol 1,4,5-trisphosphate-activated calcium release by heparin. J. Biol. Chem. 263, 11075–11079.

Goudeau, H., Goudeau, M., Guibort, N., 1992. The fertilization potential and associated membrane potential oscillations during the resumption of meiosis in the egg of the ascidian *Phallusia mammillata*. Dev. Biol. 153, 227–241.

Gould, M.C., Stephano, J.L., 2003. Polyspermy prevention in marine invertebrates. Microsc. Res. Tech. 61, 379–388.

Hirohashi, N., Vacquier, V.D., 2003. Store-operated calcium channels trigger exocytosis of the sea urchin sperm acrosomal vesicle. Biochem. Biophys. Res. Commun. 304, 285–292.

Hülser, D., Schatten, G., 1982. Bioelectric responses at fertilization. Gamete Res. 5, 363–377.

Johnson, J.D., Misler, S., 2002. Nicotinic acid-adenine dinucleotide phosphate-sensitive calcium stores initiate insulin signaling in human beta cells. Proc. Natl. Acad. Sci. U. S. A. 99, 14566–14571.

Lee, H.C., Aarhus, R., Walseth, T.F., 1993. Calcium mobilization by dual receptors during fertilization of sea urchin eggs. Science 261, 352–355.

Lee, S.J., Madden, P.J., Shen, S.S., 1998. U73122 blocked the cGMP-induced calcium release in sea urchin eggs. Exp. Cell Res. 242, 328–340.

Lim, D., Kyozuka, K., Gragnaniello, G., Carafoli, E., Santella, L., 2001. NAADP+ initiates the Ca^{2+} response during fertilization of starfish oocytes. FASEB J. 15, 2257–2267.

Lim, D., Ercolano, E., Kyozuka, K., Nusco, G.A., Moccia, F., Lange, K., Santella, L., 2003. The M-phase-promoting factor modulates the sensitivity of the Ca^{2+} stores to inositol 1,4,5-trisphosphate via the actin cytoskeleton. J. Biol. Chem. 278, 42505–42514.

Lynn, J.W., McCulloh, D.H., Chambers, E.L., 1988. Voltage clamp studies of fertilization in sea urchin eggs. II. Current patterns in relation to sperm entry, nonentry, and activation. Dev. Biol. 128, 305–323.

McCulloh, D.H., Lynn, J.W., Chambers, E.L., 1987. Membrane depolarization

facilitates sperm entry, large fertilization cone formation, and prolonged current responses in sea urchin oocytes. Dev. Biol. 124, 177–190.

McDougall, A., Gillot, I., Whitaker, M., 1993. Thimerosal reveals calcium-induced calcium release in unfertilised sea urchin eggs. Zygote 1, 35–42.

Meijer, L., Guerrier, P., 1984. Maturation and fertilization of starfish oocytes. Int. Rev. Cyt. 86, 129–196.

Miyazaki, S.I., Hirai, H., 1979. Fast polyspermy block and activation potential. Correlated changes during oocyte maturation of a starfish. Dev. Biol. 70, 327–340.

Miyazaki, S.I., Ohmori, H., Sasaki, S., 1975. Potassium rectifications of the starfish oocyte membrane and their changes during oocyte maturation. J. Physiol. 246, 55–78.

Moccia, F., Lim, D., Nusco, G.A., Ercolano, E., Santella, L., 2003a. NAADP activates a Ca^{2+} current that is dependent on F-actin cytoskeleton. FASEB J. 17, 1907–1909.

Moccia, F., Nusco, G.A., Lim, D., Ercolano, E., Gragnaniello, G., Brown, E.R., Santella, L., 2003b. Ca^{2+} signalling and membrane current activated by cADPr in starfish oocytes. Pfluegers Arch. 446, 541–552.

Moccia, F., Lim, D., Kyozuka, K., Santella, L., 2004. NAADP triggers the fertilization potential in starfish oocytes. Cell Calcium 36, 515–524.

Moody, W.J., Lansman, J., 1983. Developmental regulation of Ca^{2+} and K^{+} currents during hormone-induced maturation of starfish oocytes. Proc. Natl. Acad. Sci. 80, 3096–3100.

Nusco, G.A., Lim, D., Sabala, P., Santella, L., 2002. Ca^{2+} response to cADPr during maturation and fertilization of starfish oocytes. Biochem. Biophys. Res. Commun. 290, 1015–1021.

Patel, S., 2004. NAADP-induced Ca^{2+} release—A new signalling pathway. Biol. Cell 96, 19–28.

Rhee, S.G., 2001. Regulation of phosphoinositide-specific phospholipase C. Annu. Rev. Biochem. 70, 281–312.

Runft, L.L., Jaffe, L.A., Mehlmann, L.M., 2002. Egg activation at fertilization: where it all begins. Dev. Biol. 245, 237–254.

Runft, L.L., Carroll, D.J., Gillet, J., Giusti, A.F., O'Neill, F.J., Foltz, K.R., 2004. Identification of a starfish egg PLC-γ that regulates Ca^{2+} release at fertilization. Dev. Biol. 269, 220–236.

Santella, L., 2005. NAADP: a new second messenger comes of age. Mol. Interv. 5, 70–72.

Santella, L., Kyozuka, K., 1994. Reinitiation of meiosis in starfish oocytes requires an increase in nuclear Ca^{2+}. Biochem. Biophys. Res. Commun. 203, 674–680.

Santella, L., De Riso, L., Gragnaniello, G., Kyozuka, K., 1999. Cortical granule translocation during maturation of starfish oocytes requires cytoskeletal rearrangement triggered by InsP3-mediated Ca^{2+} release. Exp. Cell Res. 248, 567–574.

Santella, L., Kyozuka, K., Genazzani, A.A., De Riso, L., Carafoli, E., 2000. Nicotinic acid adenine dinucleotide phosphate-induced Ca^{2+} release. Interactions among distinct Ca^{2+} mobilizing mechanisms in starfish oocytes. J. Biol. Chem. 275, 8301–8306.

Santella, L., Lim, D., Nusco, G.A., 2002. Calcium and calcium-linked second messengers are main actors in the maturation and fertilization of starfish oocytes. In: Lee, K.W. (Ed.), Cyclic ADP-ribose and NAADP. Kluwer Academic Publishers, Dordrecht, pp. 381–396.

Santella, L., Lim, D., Moccia, F., 2004. Calcium and fertilization: the beginning of life. Trends Biochem. Sci. 29, 400–408.

Santella, L., Ercolano, E., Nusco, G.A., 2005. The cell cycle: a new entry in the field of Ca^{2+} signaling. Cell. Mol. Life Sci. 62, 2405–2413.

Stephano, J.L., Gould, M.C., 1997. The intracellular calcium increase at fertilization in *Urechis caupo* oocytes: activation without waves. Dev. Biol. 191, 53–68.

Stricker, S.A., 1995. Time-lapse confocal imaging of calcium dynamics in starfish embryos. Dev. Biol. 170, 496–518.

Stricker, S.A., 1999. Comparative biology of calcium signaling during fertilization and egg activation in animals. Dev. Biol. 211, 157–176.

Stricker, S.A., Centonze, V.E., Melendez, R.F., 1994. Calcium dynamics during starfish oocyte maturation and fertilization. Dev. Biol. 166, 34–58.

Yamasaki, M., Thomas, J.M., Churchill, G.C., Garnham, C., Lewis, A.M., Cancela, J.M., Patel, S., Galione, A., 2005. Role of NAADP and cADPR in the induction and maintenance of agonist-evoked Ca^{2+} spiking in mouse pancreatic acinar cells. Curr. Biol. 15, 874–878.